Mechanism of Tetracaine Block of Cyclic Nucleotide-gated Channels

ANTHONY A. FODOR, SHARONA E. GORDON, and WILLIAM N. ZAGOTTA

From the Department of Physiology and Biophysics, Howard Hughes Medical Institute, University of Washington School of Medicine, Seattle, Washington 98195-7290

ABSTRACT Local anesthetics are a diverse group of ion channel blockers that can be used to probe conformational changes in the pore. We examined the effects of the local anesthetic tetracaine on rod and olfactory cyclic nucleotide-gated channels expressed from subunit 1 in *Xenopus* oocytes. We found that 40 μM tetracaine effectively blocked the bovine rod channel but not the rat olfactory channel at saturating concentrations of cGMP. By testing chimeric channels containing regions of sequence from both rod and olfactory channels, we found that determinants of apparent affinity for tetracaine at saturating cGMP did not map to any one region of the channel sequence. Rather, the differences in apparent affinity could be explained by differences between the chimeras in the free energy of the opening allosteric transition. If a channel construct (such as the rod channel) spent appreciable time in the closed state at saturating cGMP, then it had a high apparent affinity for tetracaine. If, on the other hand, a channel construct (such as the olfactory channel) spent little time in the closed state at saturating cGMP, then it had a low apparent affinity for tetracaine. Furthermore, tetracaine became more effective at low concentrations of cGMP and at saturating concentrations of cAMP, conditions which permit the channels to spend more time in the closed configuration. These results were well fit by a model in which tetracaine binds more tightly to the closed channel than to the open channel. Dose-response curves for tetracaine in the presence of saturating cGMP are well fit with a Michaelis-Menten binding scheme indicating that a single tetracaine molecule is sufficient to produce block. In addition, tetracaine block is voltage dependent with an effective $z\delta$ of +0.56. These data are consistent with a pore-block hypothesis. The finding that tetracaine is a state-dependent pore blocker suggests that the inner mouth of the pore of cyclic nucleotide-gated channels undergoes a conformational change during channel opening.

KEY WORDS: local anesthetic • cGMP • cAMP • photoreceptor • olfactory receptor

INTRODUCTION

Ion channels directly gated by cyclic nucleotides translate cytoplasmic chemical events brought about by environmental stimuli into an electrical response (reviewed in Lancet, 1986; Yau and Baylor, 1989; Zufall et al., 1994). In the retinal rod, the signal transduction cascade initiated by light absorption causes a decrease in cGMP concentration, closing a cGMP-gated cation channel in the photoreceptor outer segment plasma membrane (Yau and Baylor, 1989). In olfactory receptor cells, the binding of odorant molecules initiates a transduction cascade that increases the level of cAMP and opens a cAMP-gated cation channel (Lancet, 1986; Zufall et al., 1994; Zimmerman, 1995). Although they were initially identified in sensory tissue, cyclic nucleotide-gated (CNG)[1] channels have also been found in a wide variety of tissues such as sperm, heart, kidney, and brain where their functions are less well characterized (reviewed in Zagotta and Siegelbaum, 1996; Finn et al., 1996). Although they lack pronounced voltage dependence, CNG channels exhibit sequence similarity to the voltage-gated family of ion channels in two key regions: the S4 region thought to be the voltage sensor of voltage-gated channels and the P region thought to comprise a portion of the ion-conducting pore (Jan and Jan, 1990; Heginbotham et al., 1992). Based on these similarities it appears as though the CNG channels are members of the superfamily that includes the voltage-gated Na^+, Ca^{2+}, and K^+ channels.

The similarity of CNG channels to voltage-gated channels suggests that each individual channel consists of a number of subunits which surround a common pore. Recent evidence has suggested that the channel is a tetramer (Gordon and Zagotta, 1995*c*; Liu et al., 1996; Varnum and Zagotta, 1996). Dose-response curves for activation of both rod and olfactory channels by cyclic nucleotides are typically fit with Hill slopes of greater than one suggesting that opening of the channel requires binding of cyclic nucleotide to more than one subunit (Fesenko et al., 1985; Haynes et al., 1986; Zimmerman and Baylor, 1986; Nakamura and Gold, 1987; Kaupp et al., 1989; Dhallan et al., 1990; Frings et al., 1992). These liganded subunits then undergo a concerted transformation to the open state (Karpen et al., 1988; Goulding et al., 1994; Varnum and Zagotta, 1996).

The primary subunits (Subunit 1) of the mammalian rod and olfactory channels are highly homologous to each other (~60% amino acid identity) yet when ex-

Address correspondence to William N. Zagotta, Department of Physiology and Biophysics, Howard Hughes Medical Institute, University of Washington School of Medicine, Box 357290, Seattle, WA 98195-7290. Fax: 206-543-0934; E-mail: Zagotta@u.washington.edu

[1]*Abbreviation used in this paper:* CNG, cyclic nucleotide-gated.

pressed exogenously the channels formed from these proteins have distinct properties. The rod channel is much more responsive to cGMP, its physiological ligand, than to cAMP; currents produced with saturating concentrations of cAMP are on the order of 1% as large as currents produced by saturating cGMP (Goulding et al., 1994; Gordon and Zagotta, 1995*b*). The olfactory channel, on the other hand, is responsive to both cAMP, its physiological ligand, and to cGMP. Saturating concentrations of both nucleotides produce roughly equal currents (Dhallan et al., 1990; Gordon and Zagotta, 1995*b*). While both channels exhibit a higher apparent affinity for cGMP than cAMP, the olfactory channel has higher apparent affinity for both cyclic nucleotides than does the rod channel (Altenhofen et al., 1991; Gordon and Zagotta, 1995*b*).

The differences in cAMP efficacy and cGMP apparent affinity between the rod and olfactory channels can be accounted for by differences between the two channels in the free energy of the opening allosteric transition (Goulding et al., 1994; Gordon and Zagotta, 1995*b*). cAMP for both channels is less effective than cGMP at promoting the allosteric transition to the open state. Because the olfactory channel is energetically easier to drive into the open state, however, cAMP and cGMP produce nearly equal currents in the olfactory channel.

Local anesthetics have been shown to be effective at blocking a wide variety of ion channels (Hille, 1992). Tetracaine, a member of the local anesthetic family, has been shown to have moderate affinity for the native rod channel (Schnetkamp, 1987; Schnetkamp, 1990; Ildefonse and Bennett, 1991; Quandt et al., 1991). In addition, two compounds related in structure to tetracaine, L-*cis*-diltiazem and amiloride, have been shown to block CNG channels (Koch and Kaupp, 1985; Stern et al., 1986; Schnetkamp, 1987, 1990; Ildefonse and Bennett, 1991; Quandt et al., 1991; McLatchie and Matthews, 1992; Haynes, 1992; McLatchie and Matthews, 1994). In this paper we exploit the differences in the free energy of the allosteric transition of the rod and olfactory channels to show that high affinity binding of tetracaine occurs only with the closed conformation of the pore.

METHODS

The cDNA clone for subunit 1 of the bovine rod channel was isolated as previously described (Gordon and Zagotta, 1995*a*). The amino acid sequence was identical to the published sequence (Kaupp et al., 1989). Subunit 1 of the olfactory channel was a generous gift of R.R. Reed (The Johns Hopkins School of Medicine, Baltimore, MD). The chimeras were constructed as previously described (Gordon and Zagotta, 1995*a*). The splice sites of the chimeras were located at the following positions: amino terminus, T162 (rod), W141 (olfactory); S1, A183 (rod), A162 (olfactory); S4-S5 linker, R285 (rod), R264 (olfactory); carboxy terminus, F421 (rod), F400 (olfactory). An alanine to valine substitution at position 483 (rod) was present in chimeras containing rod sequence at that position (CHM3, CHM11, CHM15, CHM18) and caused a small decrease in the apparent affinity for cGMP (data not shown).

Oocytes were injected with cRNA for subunit 1 of the bovine rod CNG channel, subunit 1 of the rat olfactory CNG channel, or the appropriate chimera. Oocytes were incubated for 3–10 d and patch-clamped in the inside-out configuration using ~500 kΩ borosilicate pipettes. Solution changes to the cytoplasmic side of the patch were made with an RSC100 rapid solution changer (Molecular Kinetics, Pullman, WA). Tetracaine and cyclic nucleotides were obtained from Sigma Chemical Co. (St. Louis, MO). Tetracaine solutions were generally used within 1 wk after being made. cGMP, cAMP, and tetracaine were added to a low-divalent NaCl solution which contained 130 mM NaCl, 3 mM HEPES, and 200 μM EDTA. All solutions were adjusted to pH 7.2 with NaOH. The pipette solution consisted of the low-divalent solution without added tetracaine or cyclic nucleotides. The leak currents in the absence of cyclic nucleotide at the corresponding voltage were subtracted from each record. All experiments were performed at room temperature (~20°C). All macroscopic currents were sampled at 50 kHz and filtered at 2 kHz. Data analysis was performed with the graphical analysis software Igor (WaveMetrics, Lake Oswego, OR).

In the absence of tetracaine, the currents at depolarized voltages exhibited a small sag due to ion accumulation or depletion as indicated by the small tail currents seen when stepping back to 0 mV (Zimmerman et al., 1988). The sag in the current was generally <10%. The error caused by ion accumulation or depletion was therefore ignored, and all currents were measured at the end of the voltage pulse to allow gating and tetracaine block to reach steady state.

The probability of the channel being in a conducting state for the model of Fig. 3 *A*, P_O, was calculated via the method previously described (Varnum and Zagotta, 1996):

$$P_o = \frac{[cG]^2 K^2 L}{\left(\begin{array}{l} 1 + 2K[cG] + [cG]^2 K^2 L + K^2 [cG]^2 + \\ \dfrac{K^2 [cG]^2 [T]}{K_{Dc}} + \dfrac{[T]}{K_{Dc}} + \dfrac{2K[cG][T]}{K_{Dc}} + \dfrac{K^2 [cG]^2 [T] L}{K_{Do}} \end{array}\right)},$$

where [cG] is the concentration of cGMP, [T] is the concentration of tetracaine, K is the equilibrium constant of the initial binding of ligand to the channel, L is the equilibrium constant of the allosteric transition from the fully liganded closed state to the open state, K_{Dc} is the disassociation constant of tetracaine binding to the closed state, and K_{Do} is the disassociation constant of tetracaine binding to the open state. Curves in Fig. 4, *B* and *C*, were generated by fits to:

$$I = P_o I_{Sat\ cGMP}\left(\frac{L+1}{L}\right),$$

where P_O is defined as above and $I_{Sat\ cGMP}$ is the current measured at saturating cGMP.

$K_{D\ cGMP}$ is defined as the concentration of cGMP that produces half the current seen at saturating cGMP in the absence of tetracaine. The model predicts:

$$K_{D\ cGMP} = \frac{1 + \sqrt{2 + L}}{K + KL}.$$

$K_{D\ Tet}$ is defined as the concentration of tetracaine that, at saturating cGMP, blocks half the current. The model predicts:

$$K_{D\ Tet} = \frac{K_{Dc} K_{Do} (1 + L)}{K_{Do} + K_{Dc} L}.$$

The fits in Fig. 3 *B* were generated by solving this equation for L and substituting into the equation for $K_{D\ cGMP}$:

$$K_{D\ cGMP} = \frac{1 + \sqrt{2 + \dfrac{K_{Do}(K_{D\ Tet} - K_{DC})}{K_{DC}(K_{DO} - K_{D\ Tet})}}}{K + K\left(\dfrac{K_{Do}(K_{D\ Tet} - K_{DC})}{K_{DC}(K_{DO} - K_{D\ Tet})}\right)}.$$

This equation assumes that all the chimeras have the same K, K_{Dc}, and K_{Do} but that each chimera has a distinct value for L. The dashed line in Fig. 3 *B* was generated by setting $K_{Do} = \infty$.

Single-channel recordings were made with a sampling frequency of 25 kHz and filtered at 4 kHz. Amplitude histograms were constructed from 30 s of continuously recorded data at +80 mV. The steady-state leak current was subtracted from the data so that the peak of the closed channel current occurred at 0 pA. The amplitude histograms were expressed as probability density functions (pdf). The histograms were then fit to an equation for the sum of Gaussian distributions. The relative area under each Gaussian was constrained to a binomial distribution describing the expected behavior of N independent and identical channels:

$$y = \frac{1}{\sqrt{2\pi}} \sum_{n=0}^{N} \binom{N}{n} \frac{P_o^{\,n} (1-P_o)^{N-n} e^{-\frac{1}{2}(x-ni)^2/(\sigma^2+n\varepsilon^2)}}{\sqrt{\sigma^2+n\varepsilon^2}}.$$

In this equation, y is the probability density of the current found at x pA, P_O is the probability of a single channel being in the open state, N is the number of channels in the patch, n is the number of channels open, $\binom{N}{n}$ is the number of ways to choose n open channels from a pool of N channels, i is the single-channel amplitude, σ is the standard deviation of the closed channel noise, and ε is the extra noise associated with the open state.

RESULTS

The mammalian rod and olfactory CNG channels were expressed by injecting cRNA's for subunit 1 into *Xenopus* oocytes, from which inside-out excised patch-clamp recordings were obtained. Fig. 1 *A* shows current responses to voltage steps from 0 mV to between −80 and +80 mV in steps of +20 mV. All of the traces in Fig. 1 *A* were obtained in the presence of a saturating concentration (2 mM) of cGMP, and the leak currents in the absence of cGMP were subtracted. The application of 40 μM tetracaine to the bath solution caused a significant block of the rod channel ($I_{Tet}/I = 0.090 \pm 0.013$, mean ± SEM, $N = 11$, currents at +60 mV) but much less block of the olfactory channel ($I_{Tet}/I = 0.84 \pm 0.026$, $N = 9$, currents at +60 mV). Tetracaine block of these channels reversed with a slow time course (data not shown). The time-dependent decrease in current at depolarized voltages and increase in current at hyperpolarized voltages seen in the presence of tetracaine reflect, respectively, voltage-dependent binding and unbinding of tetracaine to the channel (discussed in Fig. 8 below). Fig. 1 *B* shows dose-response curves for tetracaine in the presence of 2 mM cGMP. Currents were measured at the end of a 140-ms pulse to +60 mV and normalized by currents recorded from each patch in the presence of 2 mM cGMP and the absence of tetracaine. The data were fit with the Michaelis-Menten equation which describes binding of a single blocker molecule to a single binding site:

$$\frac{I_{Tet}}{I} = \frac{K_{D\,Tet}}{K_{D\,Tet} + [Tet]},$$

where I_{Tet} is the current in the presence of tetracaine, I is the current without tetracaine, $K_{D\,Tet}$ is the concentration of tetracaine which blocks half the current at +60 mV, and [Tet] is the concentration of tetracaine applied to the patch from the cytoplasmic side. This equation fit the tetracaine dose-response relations well suggesting that a single tetracaine molecule was sufficient to block these CNG channels. The rod channels had a much higher apparent affinity for tetracaine ($K_{D\,Tet} = 4.6$ μM ± 0.70 μM, mean ± SEM, $N = 11$) then did the olfactory channels ($K_{D\,Tet} = 170$ μM ± 22 μM, $N = 6$). Note that these K_D's would both be higher at more hyperpolarized potentials (see below).

In an attempt to localize the difference in tetracaine apparent affinity between the rod and olfactory chan-

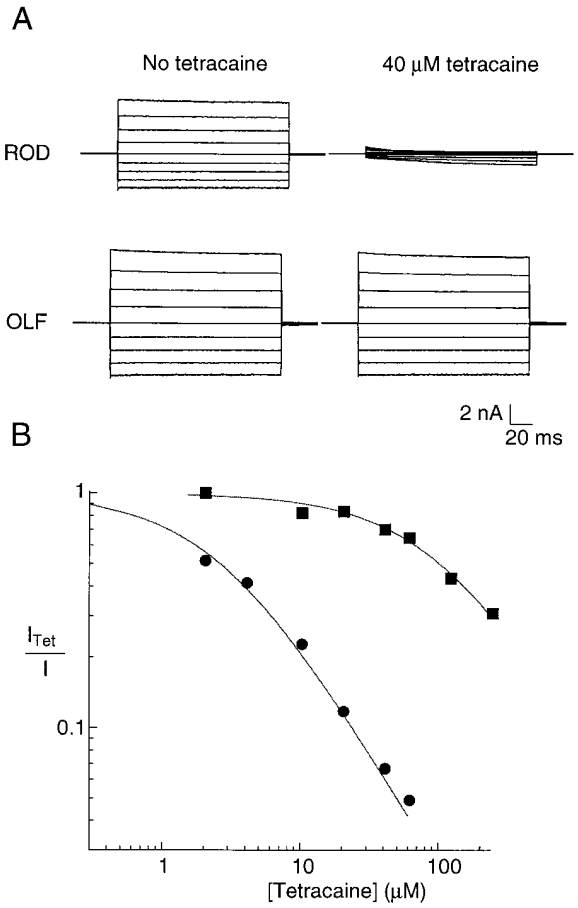

FIGURE 1. At saturating cGMP, tetracaine effectively blocks the rod but not the olfactory channel. (*A*) Current families are recorded in response to voltage steps from 0 mV to between −80 and +80 mV in 20-mV steps. The top set of traces are from the bovine rod channel and the bottom set of traces are from the rat olfactory channel. All currents were recorded in the presence of 2 mM cGMP. The left traces are in the absence of tetracaine and the right traces are in identical solutions with 40 μM tetracaine. (*B*) Dose-response curves for tetracaine block. Circles represent data from the rod channel and squares from the olfactory channel. Smooth curves are fits to the data with the Michaelis-Menten equation (see RESULTS) with $K_{D\,Tet} = 2.63$ μM for the rod channel and $K_{D\,Tet} = 102.4$ μM for the olfactory channel. All currents were measured at +60 mV.

nels, we generated chimeras between the two channel sequences. Dose-response curves for tetracaine were measured in the presence of 2 mM cGMP and apparent affinity for tetracaine ($K_{D\ Tet}$) was determined from fits with the Michaelis-Menten equation as above. The open boxes in Fig. 2 show values of $K_{D\ Tet}$ for the olfactory channel, rod channel, and 8 chimeras that contained different regions of the rod and olfactory channel sequence. For each chimera, segments of rod channel sequence are shown in gray and segments of olfactory channel sequence are shown in black. The chimeras are arranged from lowest apparent affinity for tetracaine at the top to highest apparent affinity for tetracaine at the bottom. Tetracaine apparent affinity did not appear to map to any single region of the channel. In particular, replacing the pore of the rod channel with the corresponding region of the olfactory channel did not shift the apparent affinity for tetracaine of the resulting chimera (CHM11) towards that of the olfactory channel. Tetracaine apparent affinity, however, was strongly influenced by the NH_2-terminal region. Replacing the NH_2-terminal of the rod channel with the NH_2-terminal of the olfactory channel (CHM15) decreased the apparent affinity for tetracaine by about a factor of 10 relative to the rod channel. Likewise, replacing the NH_2-terminal of the olfactory channel with that of the rod channel (CHM16) increased the apparent affinity for tetracaine by about a factor of 10 relative to the olfactory channel. In general, however, the more olfactory sequence a given chimera contained, the closer its apparent affinity for tetracaine was to the olfactory channel, and the more rod sequence a given chimera contained, the closer its apparent affinity for tetracaine was to the rod channel.

It has recently been shown that the NH_2-terminal of cyclic nucleotide-gated channels influences the free energy of the allosteric transition from the closed to the open state (Goulding et al., 1994; Gordon and Zagotta, 1995*b*). The finding that the same regions of the channel influence both the free energy of the opening allo-

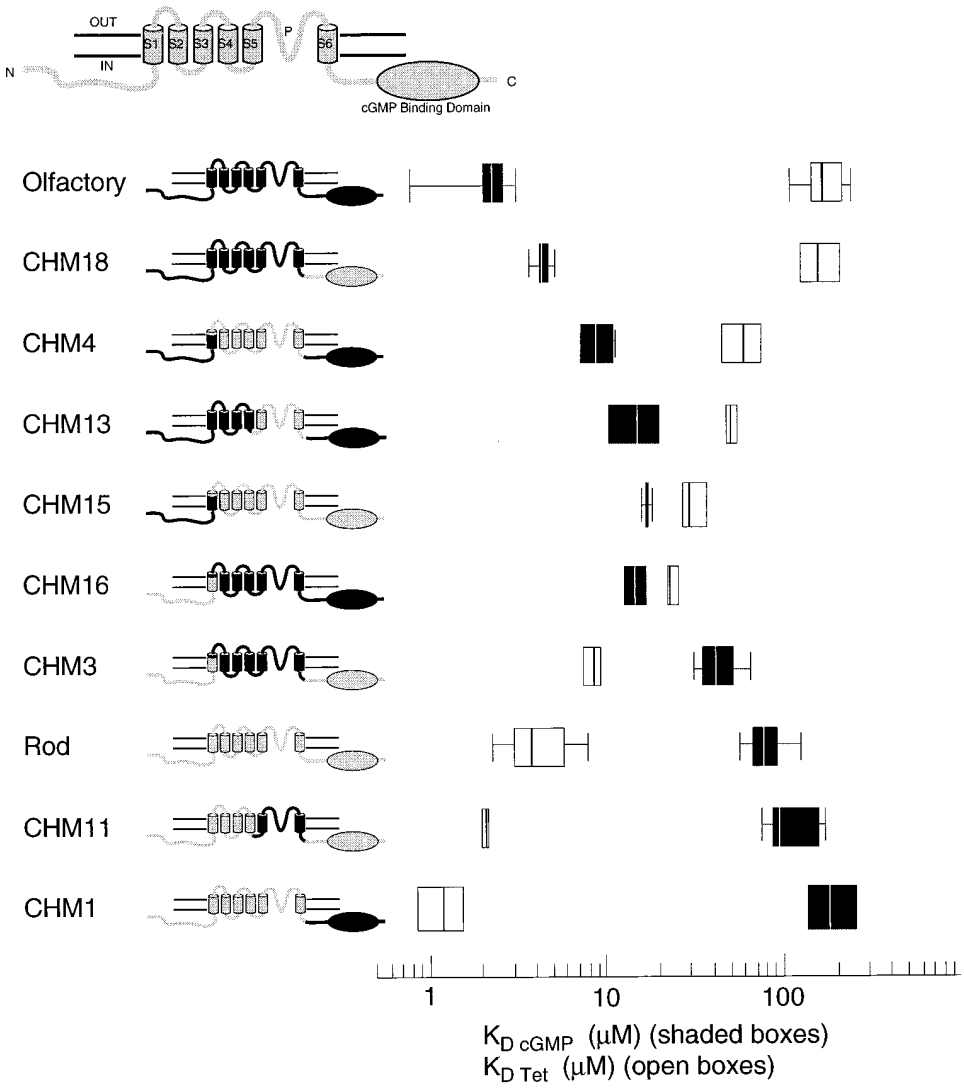

FIGURE 2. The $K_{D\ cGMP}$ for cGMP and the $K_{D\ Tet}$ for tetracaine are inversely correlated for a number of rod-olfactory channel chimeras. $K_{D\ cGMP}$'s for cGMP are indicated by shaded boxes. $K_{D\ Tet}$'s for tetracaine are indicated by open boxes. Values for $K_{D\ Tet}$ were obtained from fits to the Michaelis-Menten equation and values for $K_{D\ cGMP}$ were obtained from fits to the Hill Equation (see Results). $K_{D\ cGMP}$ is defined as the concentration of cGMP which produces half the current seen at saturating cGMP. $K_{D\ Tet}$ is defined as the concentration of tetracaine that blocks half the current at saturating cGMP. In this box plot, the left and right edges of the boxes shows the 25th and 75th percentiles of the data. The whiskers coming out of some of the boxes show the 5th and 95th percentiles. The line in the middle of the boxes shows the median.

steric transition and tetracaine apparent affinity suggests that tetracaine may block CNG channels in a state-dependent manner. To test this hypothesis, we measured dose-response relations for cGMP for all of the chimeras shown in Fig. 2. The dose-response data were fit to the Hill equation of the form:

$$I = I_{\max}\frac{[\mathrm{cGMP}]^n}{K_{D\,cGMP}^n + [\mathrm{cGMP}]^n},$$

where $I_{\max}$ is the current produced by saturating cGMP, n is the Hill slope (usually ~2 for these channels), and $K_{D\ cGMP}$ is the concentration of cGMP, that produces half of the current seen at saturating cGMP. The filled boxes in Fig. 2 show $K_{D\ cGMP}$ for each of the chimeras. As with the apparent affinity for tetracaine, the apparent affinity for cGMP did not localize to any one part of the channel (Gordon and Zagotta, 1995*b*). Rather, channels which consisted mostly of rod sequence tended to have an apparent affinity for cGMP closer to that of the rod channel whereas channels which consisted mostly of olfactory sequence tended to have an apparent affinity for cGMP closer to that of the olfactory channel. Indeed, as Fig. 2 shows, the apparent affinities for tetracaine and cGMP were inversely correlated. This inverse correlation of cGMP and tetracaine apparent affinity could be explained by both values tracking the relative stability of the allosteric transition to the open state of each chimera. As one moves from top to bottom in Fig. 2, the chimeras required a higher concentration of cGMP to activate them. In addition, as one moves from top to bottom the chimeras required a lower concentration of tetracaine to block them. The lower apparent affinity for cGMP resulted from a less stable opening allosteric transition causing channels to spend more time in the closed state at saturating cGMP (Gordon and Zagotta, 1995*b*). If the increased tetracaine efficacy also resulted from channels spending more time in the closed state, then tetracaine must bind with a higher affinity to the closed state.

To test the hypothesis that tetracaine binds preferentially to the closed state, we constructed a model for state-dependent binding of tetracaine based on a simple allosteric mechanism for the activation of CNG channels (Gordon and Zagotta, 1995*a*, *b*). In this model (Fig. 3 *A*) two independent and identical nucleotide binding steps are followed by an allosteric transition from the closed to the open state. K is the association constant of the initial binding of ligand to each subunit, and L is the equilibrium constant of the allosteric transition. This model for channel activation is an approximation of a Monod, Wyman, and Changeux model in which the channel can bind up to four molecules of cyclic nucleotide and the binding of each cyclic nucleotide further promotes the opening allosteric transition (Monod et al., 1965; Stryer, 1987; Goulding et al., 1994; Varnum and Zagotta, 1996). While the Monod, Wyman, and Changeux scheme is perhaps a more realistic model of channel activation, the model in Fig. 3 *A* was chosen because it adequately fit our data with a minimal number of free parameters. Our model envisions tetracaine as binding to all of the closed states with the same affinity (described by disassociation constant K_{Dc}) and to the open state with a different affinity (described by disassociation constant K_{Do}). Fig. 3 *B* plots the median apparent affinity for cGMP ($K_{D\ cGMP}$) for each channel construct (*filled boxes*, Fig. 2) as a function of the median apparent affinity for tetracaine ($K_{D\ Tet}$) for each chimera (*open boxes*, Fig. 2). The dashed line in Fig. 3 *B* shows a fit of the model of Fig. 3 *A* to these data where tetracaine can only bind to the closed states (i.e., where $K_{Do} = \infty$). For this fit, K and K_{Dc} are constant and only L has been allowed to vary. This model adequately fits the data in cases, such as the rod channel, where

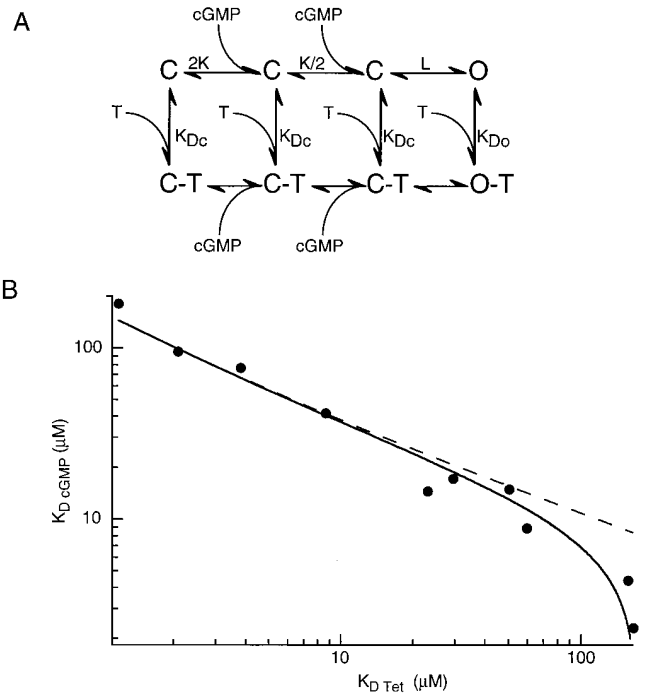

FIGURE 3. Tetracaine is a closed channel blocker. (*A*) Model of tetracaine block. K is the equilibrium constant of the initial binding of ligand to each subunit, and L is the equilibrium constant of the allosteric transition from the fully liganded closed state to the open state. T represents a tetracaine molecule which can bind to the closed states with disassociation constant K_{Dc} and the open state with disassociation constant K_{Do}. (*B*) The median values of $K_{D\ cGMP}$ plotted as a function of the median values of $K_{D\ Tet}$ for each of the chimeras in Fig. 2. The dashed line is a fit of the model with the following parameters: $K = 4{,}500\ \mathrm{M}^{-1}$, $K_{Dc} = 220$ nM, $K_{Do} = \infty$ (i.e., tetracaine can only bind to the closed state). L was varied from 5 (*leftmost point*) to 30,000 (*rightmost point*). The solid line relaxes the constraint that tetracaine can only bind to the closed state. The values for this fit are $K = 4{,}500\ \mathrm{M}^{-1}$, $K_{Dc} = 220$ nM, $K_{Do} = 170\ \mu$M, and L again varying from 5 to 30,000.

tetracaine is an effective blocker, i.e., where the channels have a low apparent affinity for cGMP and spend significant portions of their time in the closed state (Fig. 3 *B*, *leftmost points*). However, this model with block only of closed states does not adequately fit the data in cases, such as the olfactory channel, where the apparent affinity for cGMP is high and the channel spends very little time in the closed state (*rightmost points*).

Adding a parameter for open-state block (K_{Do}) gives a much better fit of the data in Fig. 3 *B* (*solid line*). For this fit, K, K_{Dc}, and K_{Do} are all constant and L varies from 5 for CHM1 (*leftmost point*, Fig. 3 *B*) to 30,000 for the olfactory channel (*rightmost point*). The fact that the model fits the data so well while varying only this one parameter (L) suggests that the differences between chimeras in both cGMP and tetracaine apparent affinity can indeed be explained by each chimera's unique value for the free energy of the allosteric transition from the closed to the open state. cGMP initially binds equally well to all the chimeras (since K is the same value for each channel construct) yet the apparent affinity for cGMP ($K_{D\ cGMP}$) varied with the energy of the allosteric transition since, as the open configuration of a channel becomes more stable, less cGMP is required to activate the channel. Likewise, tetracaine bound equally well to all the channel constructs (since K_{Dc} and K_{Do} have constant values across all chimeras), yet tetracaine apparent affinity ($K_{D\ Tet}$) varied with the energy of the allosteric transition because tetracaine binds much better to the closed state of the channel (K_{Dc} = 220 nM) than to the open state of the channel (K_{Do} = 170 μM). Since the affinity of the channels for tetracaine in the open state (K_{Do} = 170 μM) is approximately three orders of magnitude lower than the affinity of the channels for tetracaine in the closed state (K_{Dc} = 220 nM), we can conclude that tetracaine is, essentially, a closed-channel blocker.

As a more direct test of the hypothesis that tetracaine is a closed-channel blocker, we examined whether tetracaine was a more effective blocker under conditions that increase the occupancy of the channels in the closed state. We measured the effect of 4 μM tetracaine on rod and olfactory channels activated by different concentrations of cGMP (Fig. 4). At saturating concentrations (2 mM) of cGMP, 4 μM tetracaine produced little block of the olfactory channel (I_{Tet}/I = 0.96 ± 0.017, mean ± SEM, N = 4, measured at +60 mV) (Fig. 4 *A*, *top*) yet substantial block of the rod channel (0.51 ± 0.032, N = 7). At lower concentrations of cGMP, however, tetracaine became more effective at blocking both the rod (Fig. 4 *B*) and the olfactory (Figs. 4 *A*, *bottom*, and *C*) channels. The voltage-dependent time course of block of the olfactory channel (Fig 4 *A*, *bottom right*) is not as pronounced at low concentrations of cGMP and tetracaine, probably reflecting a slower blocking rate at these low concentrations. Tetracaine shifted the apparent affinity ($K_{D\ cGMP}$) of the rod channel from 83 ± 8.8 to 190 ± 17 μM (N = 7) and the $K_{D\ cGMP}$ of the olfactory channel from 2.1 ± 0.12 to 4.89 ± 0.31 μM (N = 4). The curves in Fig. 4, *B* and *C*, show fits from the model of Fig. 3 *A*.

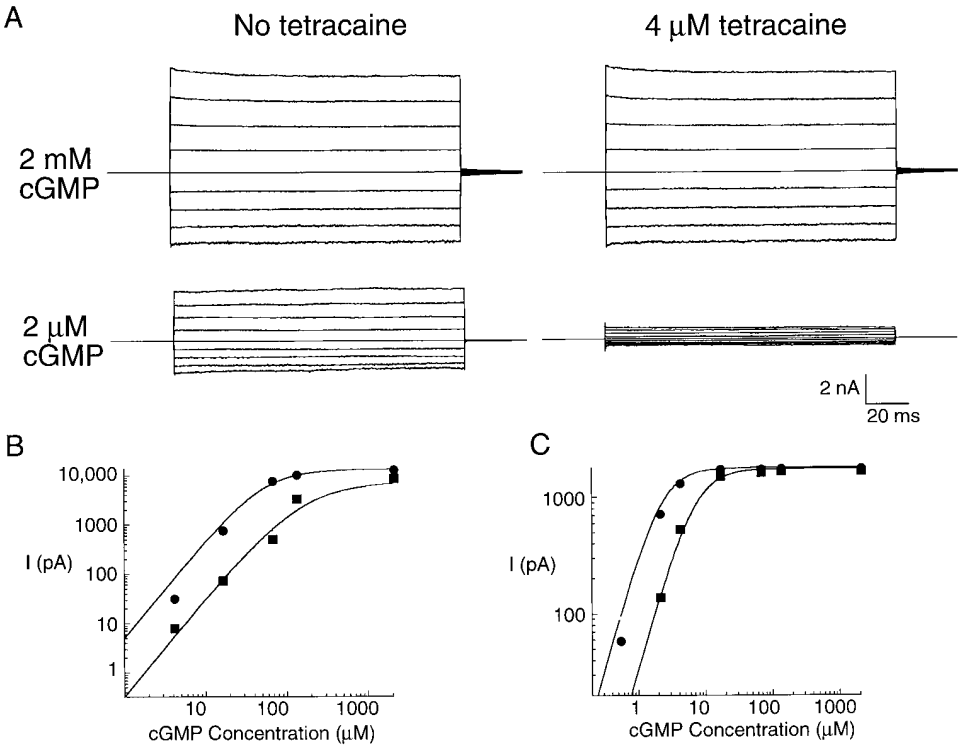

FIGURE 4. Tetracaine becomes a more effective blocker at low concentrations of cGMP. (*A*) Current traces recorded from the olfactory channel. All traces were recorded from the same patch. The top set of traces shows currents recorded at saturating cGMP in the presence and absence of 4 μM tetracaine. The bottom set of traces shows currents recorded at 2 μM cGMP in the presence and absence of 4 μM tetracaine. (*B* and *C*) cGMP dose-response curves for the rod (*B*) and olfactory (*C*) channels in the presence (*squares*) and absence (*circles*) of 4 μM tetracaine. Currents recorded at +60 mV. The curves are generated from the model in Fig. 3 *A* with the following parameters: for the rod channel, K = 4,500 M^{-1}, L = 17, K_{Dc} = 280 nM, K_{Do} = 185 μM, $I_{Sat\ cGMP}$ = 13,630 pA. For the olfactory channel: K = 4,500 M^{-1}, L = 30000, K_{Dc} = 440 nM, K_{Do} = 185 μM, $I_{Sat\ cGMP}$ = 1,781 pA. All currents were measured at +60 mV.

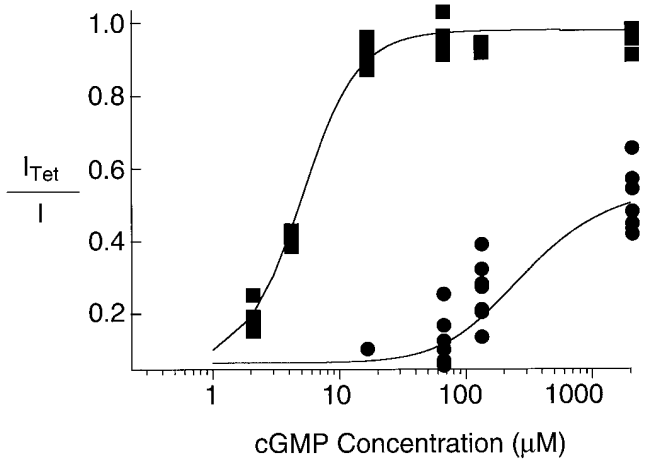

FIGURE 5. The effect of 4 μM tetracaine at different concentrations of cGMP for a number of different patches containing rod (*circles*, $N = 7$) and olfactory (*squares*, $N = 4$) channels. On the abscissa is the current recorded with 4 μM tetracaine normalized by the current recorded without tetracaine at the concentration of cGMP indicated on the ordinate. Curves are fits from the model shown in Fig. 3 *A* with the following parameters: $K = 4{,}500\ M^{-1}$, $L_{ROD} = 17$, $L_{OLF} = 30000$, $K_{Dc} = 280$ nM and $K_{Do} = 180$ μM. All currents were measured at +60 mV.

Fig. 5 shows the effect of 4 μM tetracaine on rod and olfactory channels at different concentrations of cGMP for a number of different patches. Plotted on the abscissa is current in the presence of 4 μM tetracaine normalized by the current in the absence of tetracaine at the concentration of cGMP specified on the ordinate. The effectiveness of tetracaine as a blocker was greatly increased at lower concentrations of cGMP for both the rod and the olfactory channels. As cGMP concentration was lowered and the olfactory channel spent more and more time in the closed state, tetracaine became effective at blocking the olfactory channel. This stands in contrast to results collected at saturating concentrations of cGMP, where 4 μM tetracaine produced little block of the olfactory channel. The curves in Fig. 5 show fits from the model of Fig. 3 *A*. The improved potency of tetracaine block at low concentrations of cGMP confirms that the difference in apparent affinity for tetracaine between the rod and olfactory channel seen at saturating cGMP can be accounted for by differences in the allosteric properties of the two channels.

Lowering cGMP concentration is one way to cause the olfactory channel to spend more time in the closed state. Another way is to evoke currents with saturating concentrations of cAMP, which is less effective than cGMP at promoting the transition to the open state (Gordon and Zagotta, 1995*b*). Gordon and Zagotta (1995*b*) found that, while both L_{cAMP} and L_{cGMP} are large for the olfactory channel, L_{cAMP} is significantly less than L_{cGMP}. This would cause the olfactory channel to have nearly equal currents for cAMP and cGMP but still spend significantly more time in the closed state with cAMP. For example if L_{cAMP} is 100 and L_{cGMP} is 30,000, a model like the one in Fig. 3 *A* predicts that the open probability at saturating cAMP is 0.99 and at saturating cGMP is 1.0, producing virtually identical currents. However the channel would spend 1% of its time closed at saturating cAMP, but only 0.003% of its time closed at saturating cGMP, a 300-fold difference in time spent in the closed state. We would predict, therefore, that while cAMP and cGMP produce nearly equal currents in the olfactory channel, the channels should spend more time in the closed state in the presence of saturating cAMP and should therefore be more susceptible to tetracaine's closed-channel block. Fig. 6 shows that, in

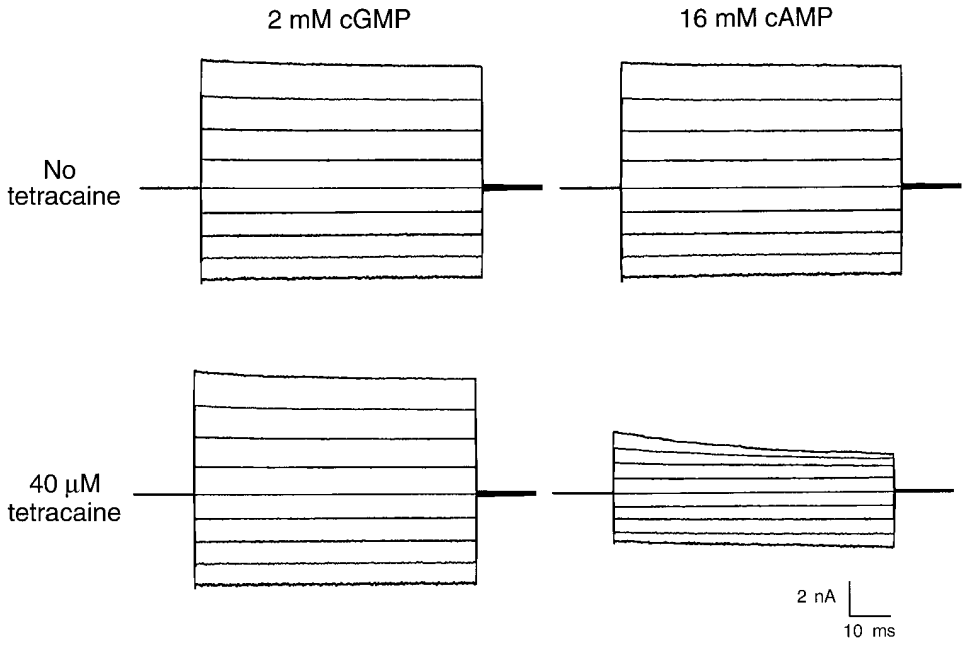

FIGURE 6. For olfactory channels, 40 μM tetracaine is more effective at blocking currents produced by saturating cAMP than for currents produced by saturating cGMP. All traces were recorded from the same patch. The top set of traces shows currents recorded in the absence of tetracaine. The bottom set of traces show currents recorded in the presence of 40 μM tetracaine. The left traces show currents evoked by a saturating concentration of cGMP while the right traces show current evoked by a saturating concentration of cAMP.

agreement with previous results (Dhallan et al., 1990; Gordon and Zagotta, 1995*b*), saturating cAMP and saturating cGMP produced approximately the same currents in the olfactory channel ($I_{\text{Sat-cAMP}}/I_{\text{Sat-cGMP}} = 0.99 \pm 0.012$ mean ± SEM, $N = 3$, measured at +60 mV). 40 μM tetracaine did not cause substantial block of currents from olfactory channels in the presence of saturating cGMP (2mM) ($I_{\text{Tet}}/I = 0.84 \pm 0.023$, $N = 9$), but, as predicted, had a much larger effect on currents in the presence of saturating cAMP ($I_{\text{Tet}}/I = 0.39 \pm 0.042$, $N = 3$). This result is consistent with both our finding that tetracaine is a closed channel blocker and with previous interpretations of why cAMP is a good ligand for the olfactory channel but not the rod channel (Goulding et al., 1994; Gordon and Zagotta, 1995*b*).

Fig. 7 shows the effect of tetracaine block on a patch containing two rod channels recorded at +80 mV and amplitude histograms constructed from 30 s of continuously recorded data. In the absence of cGMP, no openings were observed (Fig. 7 *A*). At saturating (2 mM) cGMP, both channels were open the majority of the time (Fig. 7 *B*). This is apparent in the amplitude histogram as a large peak corresponding to two channels open and a smaller peak corresponding to a single channel open. The addition of 10 μM tetracaine caused both channels to spend considerably more time in the closed state, but did not change the single-channel amplitude (Fig. 7 *C*). This is apparent as a shift in the amplitude histogram towards closed levels. The fits to the histograms of Fig. 7, *B* and *C*, are from an equation for the sum of Gaussians constrained so that the distributions of 0, 1, or 2 channels open conforms to a simple binomial distribution (see METHODS). The only difference between the fits is that P_o, the fraction of time each channel spent open, was 0.83 in the absence of tetracaine, but dropped to 0.17 in the presence of 10 μM tetracaine. The model in Fig. 3 *A* predicts that 10 μM tetracaine should block 76% of the current seen at saturating cGMP, in agreement with our single-channel data. The single-channel amplitude remained the same, 2.74 pA, in the presence and absence of tetracaine. Similar results were seen in two other patches. For all three patches, tetracaine changed the P_o from 0.75 ± 0.060 to 0.15 ± 0.01 while the single-channel amplitude in the presence of tetracaine, 2.43 ± 0.24 pA, remained indistinguishable from that in the absence of tetracaine 2.38 ± 0.22 pA. This confirms that tetracaine does not change the amplitude of single-channel currents.

The model in Fig. 3 *A* predicts that the rod channel, with an L of 17, should have a P_o of 0.94 at saturating cGMP in the absence of tetracaine. The lower P_o seen in our single-channel records in the absence of tetracaine arises from the existence of infrequent long-lived closed states (Fig. 7 *B*) not included in our model. The single-channel amplitude in our records corresponds to a single-channel conductance of ~30 pS, similar to the conductances found for native and expressed channels when recorded in the absence of divalent cations (Kaupp et al., 1989; Dhallan et al., 1990; Taylor and Baylor, 1995).

To examine the voltage dependence of tetracaine block, we recorded from rod channels in the presence

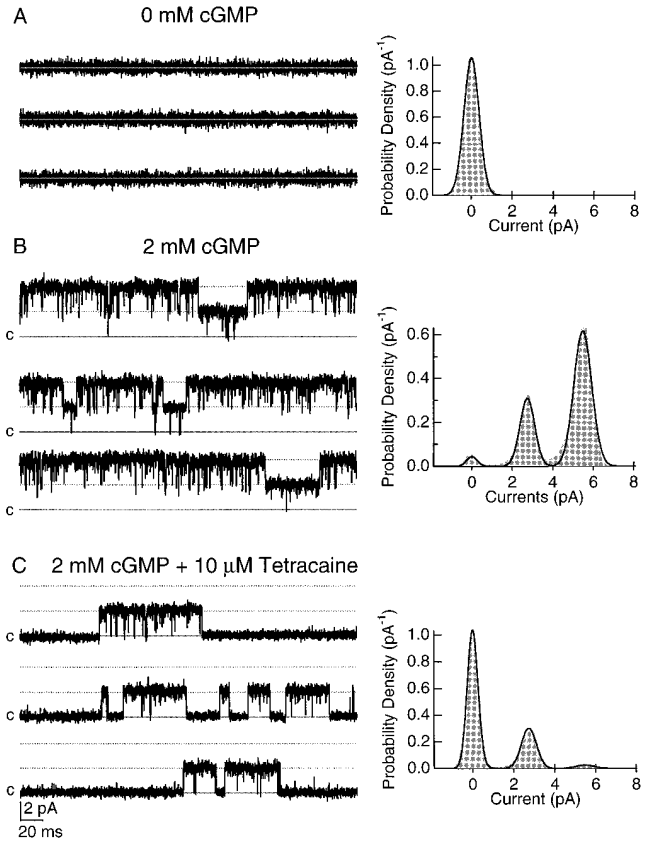

FIGURE 7. The effect of tetracaine block on single channels. All data shown are from a single patch containing two rod channels recorded at +80 mV. Amplitude histograms were constructed from 30 s of continuous recording. *c* represents the current present when both channels are closed. Dashed lines represent the currents present when one or both of the channels are open. The position of the lines representing the open states were derived from fits to the histograms and are the same in the presence and absence of tetracaine. Fits to binned data are to an equation for the sum of two Gaussians constrained so that the distribution of open channels follows a binomial distribution with $N = 2$ (see METHODS). (*A*) In the absence of cGMP, both channels are closed. Fits to the histogram are with $P_o = 0.0$ and $\sigma = 0.38$ pA. (*B*) At saturating (2 mM) cGMP, both channels spend most of their time open. Fits to the histogram are with $i = 2.74$ pA, $\sigma = 0.27$ pA, $\varepsilon = 0.25$ pA, $P_o = 0.83$. (*C*) Addition of 10 μM tetracaine causes the channels to spend less time in the open state. Fits to the histogram are with the same values as in the absence of tetracaine except that $P_o = 0.17$. Tetracaine does not cause the single-channel amplitude, *i*, to change.

of saturating cGMP (2 mM) and 40 μM tetracaine as above, but extended the time of each voltage step to 800 ms in order to allow currents at hyperpolarized voltages to achieve steady state (Fig. 8). Tetracaine block was more rapid and more pronounced at depolarized voltages. This is consistent with tetracaine being a pore blocker that binds within the membrane electric field as has been previously suggested for L-*cis*-diltiazem (McLatchie and Matthews, 1992; McLatchie and Matthews, 1994). Fig. 8 *B* shows the steady-state current recorded with tetracaine normalized by current without tetracaine at each voltage. The data is fit with the model shown in Fig. 3 *A* with K_{Do} set to infinity (i.e., only closed state binding is allowed) and K_{Dc} allowed to vary with voltage according to the following equation:

$$K_{Dc} = K_{Dc\text{-}0}\, e^{-z\delta FV/RT},$$

where $K_{Dc\text{-}0}$ is the value of K_{Dc} at 0 mV, z is the valence of the blocker (1 for tetracaine), δ is the electrical distance of the blocker in the pore, T is absolute temperature, and F and R are physical constants with their usual meaning. The equivalent charge zδ produced by such a model was 0.56 ± 0.036 ($N = 3$) suggesting that tetracaine binds approximately halfway through the membrane electric field. A similar zδ was obtained for the olfactory channel (data not shown). This value of zδ for tetracaine is almost identical to values found for the closely related blocker diltiazem (Haynes, 1992; McLatchie and Matthews, 1992), a pore blocker of rod channels (McLatchie and Matthews, 1994). The kinetics of tetracaine block also varied with voltage. Fits of each sweep with a single exponential equation show that the time constant τ varied from 153.2 ms at −80 mV to 39.27 ms at +80 mV.

It has been previously proposed that *L*, the equilibrium constant of the opening allosteric transition, is itself voltage dependent in native channels (Karpen et al., 1988). This voltage dependence in *L*, however, was described as increasing open probability at depolarized voltages and therefore can not account for the voltage dependence we see in tetracaine block. By ignoring the voltage dependence of *L*, therefore, we are, if anything, underestimating the zδ for tetracaine block.

DISCUSSION

We have exploited differences in the gating properties of the rod and olfactory channels in order to elucidate the mechanism of tetracaine block. The olfactory channel has a more stable opening allosteric transition than the rod channel and hence, at saturating cGMP, spends essentially no time in the closed state. If *L* is 30,000 for the olfactory channel, the model of Fig. 3 *A* predicts P_o is essentially 1 at saturating cGMP. Since tetracaine binds with low affinity to the open configuration, it is ineffective at blocking the olfactory channel at saturating cGMP. The rod channel has a much less favorable opening allosteric transition and spends significant time in the closed state at saturating cGMP (Gordon and Zagotta, 1995*b*). If *L* is 17 for the rod channel, the

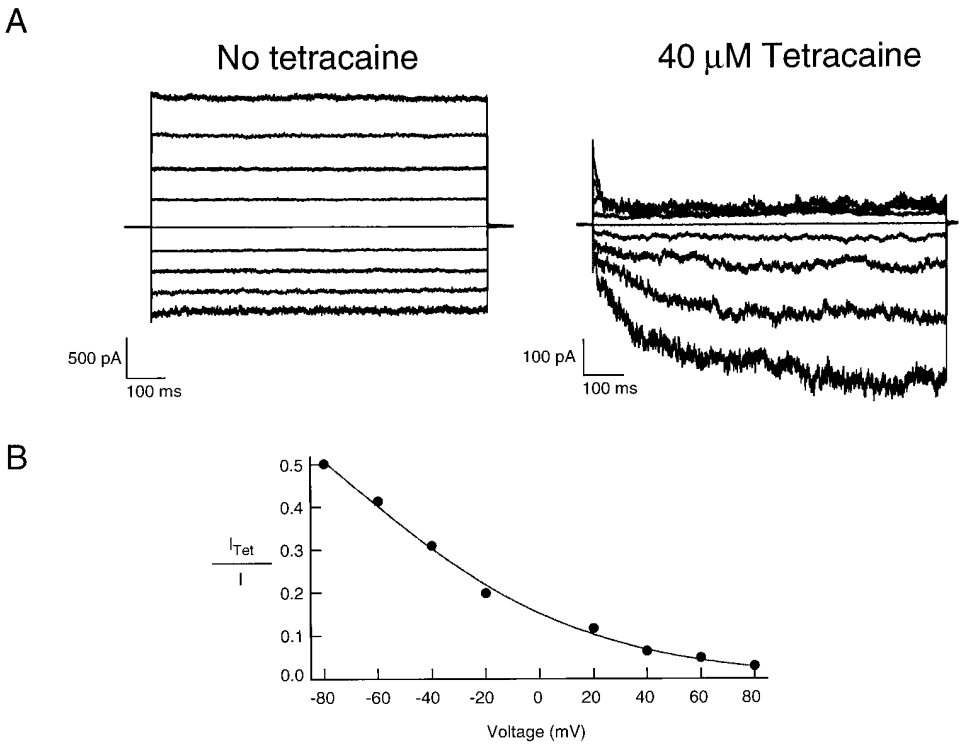

FIGURE 8. The voltage dependence of tetracaine block. (*A*) Current families recorded from the rod channels in the presence of saturating cGMP (2 mM) in response to voltage steps from 0 mV to between −80 and +80 mV in 20 mV steps. In these recordings, the duration of each voltage step was extended to 800 ms in order to allow currents from hyperpolarized voltages to achieve steady state. All data were recorded from the same patch. (*B*) The current in the presence of 40 μM tetracaine at each voltage was normalized by the current recorded in the absence of tetracaine at that voltage. The curve is a fit from the model in Fig. 3 *A* except that K_{Dc} was replaced with an expression that varied with voltage (see RESULTS). Parameters from the fit are $K_{Dc\text{-}0}$ = 365 nM, zδ = 0.56 and L = 20.

model of Fig. 3 *A* predicts P_o is 0.94 at saturating cGMP. The model predicts, therefore, that at saturating cGMP, the channel spends 6% of its time closed for the rod channel but essentially no time closed for the olfactory channel. The fully liganded rod channel is therefore much more susceptible to tetracaine's closed-channel block than is the fully liganded olfactory channel. One can make tetracaine a more effective blocker for the olfactory channel by simply increasing the amount of time the channel spends in closed states (Figs. 4–6). This suggests that the differences in tetracaine apparent affinity between the rod and the olfactory channel are due almost entirely to differences between the two channels in the free energy of the opening allosteric transition.

In previous work, single-channel analysis, the degree of Ni^{2+} potentiation, noise analysis, and open-channel block produced by Shaker NH_2-terminal inactivation ball peptide have all been used to measure how well saturating cGMP opens CNG channels (Goulding et al., 1994; Gordon and Zagotta, 1995*b*; Taylor and Baylor, 1995). These measurements allow calculation of the free energy of the allosteric transition from the closed to the open state. By granting the ability to monitor the fraction of time a channel spends in the closed state, tetracaine apparent affinity provides an independent measure of this value.

Like tetracaine, the divalent cation Ni^{2+} has been found to inhibit the olfactory channel by binding preferentially to closed states of the channel (Gordon and Zagotta, 1995*b*). The binding site for Ni^{2+} has been localized to a single histidine residue (H396) in the region following the S6 transmembrane segment, outside the putative pore domain. This raises the possibility that weak binding of Ni^{2+} to the open state does not produce channel block as it does for tetracaine.

A number of other blockers have been found to be effective on CNG channels. In particular, L-*cis*-diltiazem has been found to block CNG channels with high affinity (Koch and Kaupp, 1985; Stern et al., 1986; Schnetkamp, 1987; Schnetkamp, 1990; Ildefonse and Bennett, 1991; Quandt et al., 1991; Haynes, 1992; McLatchie and Matthews, 1992; McLatchie and Matthews, 1994). Diltiazem and tetracaine have similar structures. Both have a protonatable amine group on one end and a hydrophobic group with aromatic rings on the other which makes them lipid soluble (Fig. 9 *A*). Diltiazem block of the native rod channel has been shown to be pH dependent indicating that the charged amine group is required for block (McLatchie and Matthews, 1992, 1994), although this result has been controversial (Haynes, 1992). Diltiazem and tetracaine block have a similar voltage dependence. Like tetracaine, diltiazem becomes more effective at depolarized voltages. We report here that zδ for tetracaine = 0.56 whereas zδ values reported for diltiazem range from 0.43 (Haynes, 1992) to 0.50 (McLatchie and Matthews, 1992). The similarity in voltage dependence suggests that the binding sites for tetracaine and diltiazem are very close to one another in the pore. It should be mentioned, however, that native CNG channels have an additional subunit, subunit 2 (Chen et al., 1993). Tetracaine may have a different mechanism for block of heteromultimeric channels composed of subunits 1 and 2 than the closed-channel block we have described for channels composed only of subunit 1.

We have shown evidence that tetracaine is both a closed-state blocker and a pore blocker. The existence of a state-dependent pore blocker suggests that the pore of CNG channels undergoes a conformational

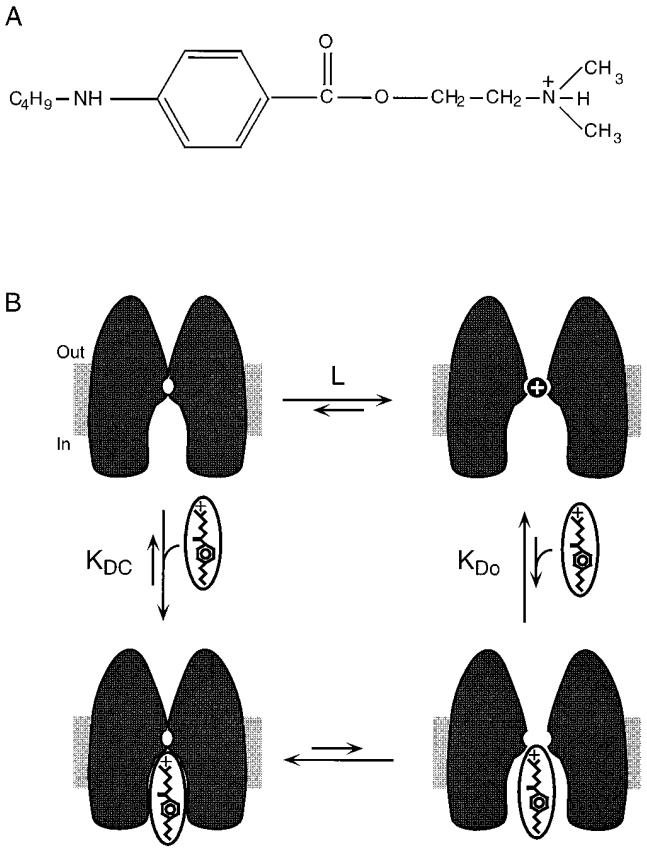

FIGURE 9. (*A*) Structure of tetracaine. (*B*) Model of tetracaine block. The greater affinity of tetracaine for closed channels is envisioned as arising from two distinct mechanisms. Interactions between tetracaine and the inner mouth of the channel pore are seen as leading to tighter binding of tetracaine to closed channels and therefore to stabilization of the closed state. An increase in the width of the pore in the open conformation disrupts these interactions leading to the lower affinity of the open state for the blocker. In addition, the open channel is seen as containing an ion in the pore, not present in the closed channel, which stabilizes the open state. The positively charged ion electrostatically repels tetracaine's positively charged amine group causing tetracaine to bind to the open state with low affinity.

change during channel opening. A cartoon of tetracaine block is shown in Fig. 9 *B*. Tetracaine block is shown for both closed and open channels. The greater affinity of tetracaine for closed channels could arise by at least two different mechanisms. Interactions between tetracaine and the inner mouth of the channel pore could lead to tighter binding of tetracaine to closed channels and therefore to stabilization of the closed state. An increase in the width of the pore in the open conformation could disrupt these interactions leading to the lower affinity of the open state for the blocker. Alternatively, the open channel may contain an ion in the pore, not present in the closed channel, which stabilizes the open state. The positively charged ion could electrostatically repel tetracaine's positively charged amine group causing tetracaine to bind to the open state with low affinity. This mechanism has been shown to account for the increased rate of C-type inactivation in voltage-dependent K^+ channels in the presence of TEA derivatives (Baukrowitz and Yellen, 1996). In addition, tetracaine has been shown to be a state-dependent blocker in Na^+ channels having a high affinity for the inactivated state (Wang et al., 1994). This raises the possibility that the closed state of CNG channels and the inactivated state of voltage-gated channels are conformationally related.

We thank R.R. Reed for the rat olfactory cDNA clone, and E.R. Liman for the high expression vector, and Elizabeth Sunderman for her help with single-channel analysis. In addition, we thank Kevin Black, Gay Sheridan, and Heidi Utsugi for technical assistance and Peter Detwiler for comments on the manuscript.

This work was supported by a grant from the National Eye Institute (EY 10329 to W.N. Zagotta) and the Human Frontiers Science Program. W.N. Zagotta is an Investigator and S.E. Gordon is an Associate of the Howard Hughes Medical Institute.

Original version received 3 July 1996 and accepted version received 24 September 1996.

REFERENCES

Altenhofen, W., J. Ludwig, E. Eismann, W. Kraus, W. Bonigk, and U.B. Kaupp. 1991. Control of ligand specificity in cyclic nucleotide-gated channels from rod photoreceptors and olfactory epithelium. *Proc. Natl. Acad. Sci. USA*. 88:9868–9872.

Baukrowitz, T., and G. Yellen. 1996. Use-dependent blockers and exit rate of the last ion from the multi-ion pore of a K^+ channel. *Science (Wash. DC)*. 271:653–656.

Chen, T.Y., Y.W. Peng, R.S. Dhallan, B. Ahamed, R.R. Reed, and K.W. Yau. 1993. A new subunit of the cyclic nucleotide-gated cation channel in retinal rods. *Nature (Lond.)*. 362:764–767.

Dhallan, R.S., K.W. Yau, K.A. Schrader, and R.R. Reed. 1990. Primary structure and functional expression of a cyclic nucleotide-activated channel from olfactory neurons. *Nature (Lond.)*. 347: 184–187.

Fesenko, E.E., S.S. Kolesnikov, and A.L. Lyubarsky. 1985. Induction by cyclic GMP of cationic conductance in plasma membrane of retinal rod outer segment. *Nature (Lond.)*. 313:310–313.

Finn, J.T., M.E. Grunwald, and K.W. Yau. 1996. Cyclic nucleotide gated channels: an extended family with diverse functions. *Annu. Rev. Physiol.* 58:395–426.

Frings, S., J.W. Lynch, and B. Lindemann. 1992. Properties of cyclic nucleotide-gated channels mediating olfactory transduction. Activation, selectivity, and blockage. *J. Gen. Physiol.* 100:45–67.

Gordon, S.E., and W.N. Zagotta. 1995*a*. A histidine residue associated with the gate of the cyclic nucleotide-activated channels in rod photoreceptors. *Neuron*. 14:177–183.

Gordon, S.E., and W.N. Zagotta. 1995*b*. Localization of regions affecting an allosteric transition in cyclic nucleotide-activated channels. *Neuron*. 14:857–864.

Gordon, S.E., and W.N. Zagotta. 1995*c*. Subunit interactions in coordination of Ni^{2+} in cyclic nucleotide-gated channels. *Proc Natl Acad Sci USA*. 92:10222–10226.

Goulding, E.H., G.R. Tibbs, and S.A. Siegelbaum. 1994. Molecular mechanism of cyclic-nucleotide-gated channel activation. *Nature (Lond.)*. 372:369–374.

Haynes, L.W. 1992. Block of the cyclic GMP-gated channel of vertebrate rod and cone photoreceptors by L-*cis*-diltiazem. *J. Gen. Physiol.* 100:783–801.

Haynes, L.W., A.R. Kay, and K.W. Yau. 1986. Single cyclic GMP-activated channel activity in excised patches of rod outer segment membrane. *Nature (Lond.)*. 321:66–70.

Heginbotham, L., T. Abramson, and R. MacKinnon. 1992. A functional connection between the pores of distantly related ion channels as revealed by mutant K^+ channels. *Science (Wash. DC)*. 258:1152–1155.

Hille, B. 1992. Ionic Channels of Excitable Membranes. 2nd ed. Sinauer Associates Inc. Sunderland, MA. 607 pp.

Ildefonse, M., and N. Bennett. 1991. Single-channel study of the cGMP-dependent conductance of retinal rods from incorporation of native vesicles into planar lipid bilayers. *J. Membr. Biol.* 123:133–147.

Jan, L.Y., and Y.N. Jan. 1990. A superfamily of ion channels. *Nature (Lond.)*. 345:672.

Karpen, J.W., A.L. Zimmerman, L. Stryer, and D.A. Baylor. 1988. Gating kinetics of the cyclic-GMP-activated channel of retinal rods: flash photolysis and voltage-jump studies. *Proc. Natl. Acad. Sci. USA*. 85:1287–1291.

Kaupp, U.B., T. Niidome, T. Tanabe, S. Terada, W. Bonigk, W. Stuhmer, N.J. Cook, K. Kangawa, H. Matsuo, T. Hirose, et al. 1989. Primary structure and functional expression from complementary DNA of the rod photoreceptor cyclic GMP-gated channel. *Nature (Lond.)*. 342:762–766.

Koch, K.W., and U.B. Kaupp. 1985. Cyclic GMP directly regulates a cation conductance in membranes of bovine rods by a cooperative mechanism. *J. Biol. Chem.* 260:6788–6800.

Lancet, D. 1986. Vertebrate olfactory reception. *Annu. Rev. Neurosci.* 9:329–355.

Liu, D.T., G.R. Tibbs, and S.A. Siegelbaum. 1996. Subunit stoichiometry of cyclic nucleotide-gated channels and effects on subunit order on channel function. *Neuron*. 16:983–990.

McLatchie, L.M., and H.R. Matthews. 1992. Voltage-dependent block by L-cis-diltiazem of the cyclic GMP-activated conductance

of salamander rods. *Proc. R. Soc. Lond. B Biol. Sci.* 247:113–119.

McLatchie, L.M., and H.R. Matthews. 1994. The effect of pH on the block by L-cis-diltiazem and amiloride of the cyclic GMP-activated conductance of salamander rods. *Proc. R. Soc. Lond. B Biol. Sci.* 255:231–236.

Monod, J., J. Wyman, and J.P. Changeux. 1965. On the nature of allosteric transitions: a plausible model. *J. Mol. Biol.* 12:88–118.

Nakamura, T., and G.H. Gold. 1987. A cyclic nucleotide-gated conductance in olfactory receptor cilia. *Nature (Lond.).* 325:442–444.

Quandt, F.N., G.D. Nicol, and P.P. Schnetkamp. 1991. Voltage-dependent gating and block of the cyclic-GMP-dependent current in bovine rod outer segments. *Neuroscience.* 42:629–638.

Schnetkamp, P.P. 1987. Sodium ions selectively eliminate the fast component of guanosine cyclic 3′,5′-phosphate induced Ca^{2+} release from bovine rod outer segment disks. *Biochemistry.* 26:3249–3253.

Schnetkamp, P.P. 1990. Cation selectivity of and cation binding to the cGMP-dependent channel in bovine rod outer segment membranes. *J. Gen. Physiol.* 96:517–534.

Stern, J.H., U.B. Kaupp, and P.R. MacLeish. 1986. Control of the light-regulated current in rod photoreceptors by cyclic GMP, calcium, and L-cis-diltiazem. *Proc. Natl. Acad. Sci. USA.* 83:1163–1167.

Stryer, L. 1987. Visual transduction: design and recurring motifs. *Chem. Scr.* 27B:161–171.

Taylor, W.R., and D.A. Baylor. 1995. Conductance and kinetics of single cGMP-activated channels in salamander rod outer segments. *J. Physiol. (Lond.).* 483:567–582.

Varnum, M.D., and W.N. Zagotta. 1996. Subunit interactions in the activation of cyclic nucleotide-gated channels. *Biophys. J.* 70: 2667–2679.

Wang, G.K., W.M. Mok, and S.Y. Wang. 1994. Charged tetracaine as an inactivation enhancer in batrachotoxin-modified Na^+ channels. *Biophys. J.* 67:1851–1860.

Yau, K.W., and D.A. Baylor. 1989. Cyclic GMP-activated conductance of retinal photoreceptor cells. *Annu. Rev. Neurosci.* 12:289–327.

Zagotta, W.N., and S.A. Siegelbaum. 1996. Structure and function of cyclic nucleotide-gated channels. *Annu. Rev. Neurosci.* 19:235–263.

Zimmerman, A.L. 1995. Cyclic nucleotide gated channels. *Curr. Opin. Neurobiol.* 5:296–303.

Zimmerman, A.L., and D.A. Baylor. 1986. Cyclic GMP-sensitive conductance of retinal rods consists of aqueous pores. *Nature (Lond.).* 321:70–72.

Zimmerman, A.L., J.W. Karpen, and D.A. Baylor. 1988. Hindered diffusion in excised membrane patches from retinal rod outer segments. *Biophys. J.* 54:351–355.

Zufall, F., S. Firestein, and G.M. Shepherd. 1994. Cyclic nucleotide-gated ion channels and sensory transduction in olfactory receptor neurons. *Annu Rev Biophys Biomol Struct.* 23:577–607.